PROCEEDINGS OF SCIENCE

Lattice gauge theory treatment of strongly correlated Dirac semimetals

Yasufumi Araki*
Institute for Materials Research, Tohoku University, Sendai 980-8577, Japan
Frontier Research Institute for Interdisciplinary Sciences, Tohoku University, Sendai 980-8578, Japan
E-mail: araki@imr.tohoku.ac.jp

We observe the effect of Coulomb interaction in three-dimensional Dirac semimetals in the strong-coupling limit. Model of the system is constructed in terms of lattice gauge theory, with the Coulomb interaction mediated by U(1) gauge field defined on the lattice. We improve the formulation by introducing a field of positive background charge, and extrapolate our analysis to the "continuous-time" limit, where the lattice spacing in the imaginary-time direction reaches zero. We find that the system in the strong-coupling limit reduces to a strongly coupled repulsive Hubbard model, which favors charge neutrality for each lattice site, turning the system into a Mott insulator. We also evaluate the discretization error, to give a proper understanding of the effective model obtained by strong-coupling expansion.

The 33rd International Symposium on Lattice Field Theory
14 -18 July 2015
*Kobe International Conference Center, Kobe, Japan**

*Speaker.

PoS(LATTICE 2015)046

1. Introduction

Dirac semimetal, which shows a doubly degenerate Dirac cone structure protected by time-reversal and spatial inversion symmetry [1], has now been attracting a great interest as a material to realize various theoretically nontrivial ideas for future applications. Graphene is a well-known example of two-dimensional (2D) Dirac semimetals, which was successfully synthesized in early 2000s [2] and is now being intensely observed both theoretically and experimentally. In three-dimensions (3D), on the other hand, the history of Dirac semimetal is quite new; it was first synthesized in Na_3Bi [3] and Cd_3As_2 [4] in 2014. The physical importance of 3D Dirac semimetals is even larger than that in 2D, since it can evolve into various novel topological phases, such as Weyl semimetals, topological insulators, axionic insulators, etc., by controlling the symmetries of the system. The physical properties of 3D Dirac semimetals are now widely studied, and experiments have shown some nontrivial properties characteristic to Dirac semimetals, such as the anomaly-induced negative magnetoresistance in $ZrTe_5$ [5].

It is possible that electron-electron interaction, such as Coulomb interaction, can change the above properties of Dirac semimetals. Since the Fermi velocity v_F of electrons is slower than the velocity of photons, namely the speed of light c, the electrons feel an effectively strong Coulomb interaction enhanced by the factor of c/v_F at the classical level, which might make the many-body effect non-negligible. Many-body effect can modify the electronic properties in Dirac semimetals, such as Fermi velocity; renormalization of Fermi velocity has long been discussed and recently been observed in the context of graphene, showing a strong enhancement of Fermi velocity around the Dirac points [6].

If the many-body effect is strong enough, it is also possible to induce spontaneous opening of a bandgap in the Dirac spectrum, turning the system into a Mott insulator. Such a spontaneous gap generation is analogous to the quark mass generation mechanism in early universe, where the chiral symmetry of quarks gets spontaneously broken under the strong interaction in quantum chromodynamics (QCD). There have been various theoretical studies on many-body effects in Dirac semimetals in terms of quantum electrodynamics (QED), based on such an analogy; in 3D Dirac semimetals, there have been perturbative analysis based on weak-coupling expansion [7], renormalization group (RG) analysis using many-flavor (large-N) approximation [8], lattice gauge theory analysis with strong-coupling expansion [9], etc. The lattice strong-coupling analysis suggests that the presence or absence of spontaneous gap generation would depend on the dimensionality of the system, even in the strong-coupling limit of the Coulomb interaction, while leaving its physical origin as an open question.

In this work, we improve the lattice strong-coupling expansion technique employed in Ref. [9]. We take into account arbitrariness of the lattice spacing discretized in the temporal direction, to evaluate the discretization error and to extrapolate our strong-coupling analysis to the continuous-time limit. We also introduce the background charge field, corresponding to the positive ions sitting at each lattice site, to account for the overall charge neutrality. As a result, we find that the Mott insulator phase is reached in the strong-coupling limit, irrespective of spatial dimensionality, due to the local charge neutrality required by the suppression of photon propagation. We show that the suppression of bandgap in the strong-coupling limit shown in the previous analysis is an artifact of the discretization of imaginary time.

2. Model

We start from the Hamiltonian of Dirac fermions sitting on a square lattice, given by

$$H_F^0 = t\sum_{\mathbf{r},j,f}\eta_j(\mathbf{r})\left[\psi_f^\dagger(\mathbf{r})\psi_f(\mathbf{r}+a\hat{j})+\text{H.c.}\right]-\mu_{\text{bg}}\sum_{\mathbf{r}}b^\dagger(\mathbf{r})b(\mathbf{r}), \tag{2.1}$$

which is the Hamiltonian form of the "staggered fermion" in the context of lattice fermion formalism. Here $\mathbf{r}=(r_1,\ldots,r_d)$ is the position of a lattice site with the spacing a, j runs over the spatial dimensions from 1 to d, and $\hat{j}$ is the unit vector along the j-axis. t is the hopping amplitude, with the staggered phase factor η_j defined by $\eta_1(\mathbf{r})=0,\quad \eta_{j\geq 2}(\mathbf{r})=(-1)^{r_1/a+\cdots r_{j-1}/a}$. $\psi_f^{(\dagger)}(\mathbf{r})$ is the annihilation (creation) operator of an electron with "flavor" f at site $\mathbf{r}$, and the eigenvalues for the electron sector are given in the momentum space as $E(\mathbf{k})=2t\sqrt{\sum_j\cos^2(ak_j)}$. These bands show the Dirac cone structure with the slope (Fermi velocity) $v_F=2at$ around 2^d points in the momentum space, $\mathbf{K}_{\nu_1\cdots\nu_d}=(\pi/2a)(\nu_1,\cdots,\nu_d)$, where each of ν_j takes the value either $+1$ or -1.

Here we have also introduced the field of background charge $b^{(\dagger)}$, representing the positive ions sitting on the lattice sites, to ensure the overall charge neutrality of the system, since nonzero total charge leads to divergence of the total Coulomb energy. If the number of flavor f is 2, such as spin-$1/2$ degrees of freedom, and the Fermi level is at the Dirac points, we need a single species of this background field to cancel the total charge. The background chemical potential μ_{bg} is set deeply under the Fermi level, so that those ions should be bound at each site.

Now we recast the partition function $Z=\text{Tr}e^{-\beta H_F}$ in path-integral formalism, following the conventional procedure: by splitting the imaginary time $\tau\in[0,\beta)$ into infinitely small time-slices $a_\tau=\beta/N_\tau$ and inserting the complete system formed by the fermion coherent states, we obtain the lattice action

$$S_F^0[\psi^\dagger,\psi;b^\dagger,b]=a_\tau\sum_{\mathbf{r},\tau}\left[\sum_f\psi_f^\dagger(\mathbf{r},\tau)\partial_\tau^+\psi_f(\mathbf{r},\tau)+b^\dagger(\mathbf{r},\tau)(\partial_\tau^+-\mu_{\text{bg}})b(\mathbf{r},\tau)\right]+a_\tau\sum_\tau H_F^0(\tau) \tag{2.2}$$

The temporal lattice spacing a_τ is independent of the spatial one a, and it should be taken infinitely small so that the path integral should be well defined. Here we first take a_τ finite, and take the continuous-time limit $a_\tau\to 0$ after the strong-coupling expansion treatment shown below.

As a consequence of this construction procedure, we use the forward difference $\partial_\tau^+\xi(\tau)\equiv[\xi(\tau+a_\tau)-\xi(\tau)]/a_\tau$, instead of the forward-backward difference like $[\chi^\dagger(\tau)\chi(\tau+a_\tau)-\chi^\dagger(\tau+a_\tau)\chi(\tau)]/2a_\tau$ appearing in the staggered formalism. The kernel of this forward difference can be diagonalized as $K(\omega_n)=e^{-i\omega_n a_\tau}-1$, by using the fermionic Matsubara frequency

$$\omega_n=\frac{2\pi}{\beta}\left(n+\frac{1}{2}\right)=\frac{2\pi}{a_\tau}\frac{n+1/2}{N_\tau}.\quad(n=0,1,\ldots N_\tau-1) \tag{2.3}$$

Since this kernel shows only the trivial zero-point $K(\omega=0)=0$ in the momentum (frequency) space, we can avoid the doubling in the temporal direction and can use the original "flavor" degrees of freedom without reducing them to match the number of flavors [1].

Based on this lattice fermion model, we introduce the Coulomb interaction mediated by the electromagnetic field, namely the U(1) gauge field. Since the velocity of the fermions is much

[1] This does not violate the Nielsen–Ninomiya's theorem, since the kernel matrix here is not (anti-)Hermitian.

slower than the speed of light, e.g. $v_F = 1.3 \times 10^6 \mathrm{m/s}$ in Cd_3As_2, we can ignore the retardation effect of the electromagnetic field, given by the spatial components of the gauge potential [2]. Thus we only need the dynamics of the scalar potential A_0, and its minimal coupling to the fermionic fields is given by $\delta S_F = -i \int d\tau \sum_{\mathbf{r}} A_0 [\sum_f \psi_f^\dagger \psi - b^\dagger b]$ in the continuous-time limit.

In the U(1)-compact formalism, the gauge variable is defined by $U_0(\mathbf{r},\tau) = \exp[i a_\tau A_0(\mathbf{r},\tau)]$. Since A_0 is coupled to the local charge density in the continuous-time limit, we define the compact gauge variables not on the lattice links, but on each lattice site. In order to avoid the discretization error up to $O(a_\tau^2 A_0^2)$, the discretized minimal coupling part should be

$$\delta S_F[\psi^\dagger, \psi; b^\dagger, b; U_0] = \sum_{\mathbf{r},\tau} \frac{U_0 - U_0^\dagger}{2} \left[\sum_f \psi_f^\dagger \psi_f - b^\dagger b \right]. \tag{2.4}$$

Since we are interested in the strong-coupling limit $g^2 \to \infty$, we neglect the gauge dynamics part, given by $S_G = (2g^2)^{-1} \int d\tau d^3\mathbf{r} (\nabla A_0)^2$ in the continuum limit.

3. Strong-coupling analysis

Now we are ready to analyze the electron correlation properties, using the lattice model constructed above. Since the gauge dynamics S_G is neglected in the strong-coupling limit $g^{-2} = 0$, the photon field U_0 does not propagate spatially. Thus the gauge field correlates the charge densities only at the same lattice site; integrating out the gauge variables U_0, we obtain an effective action for fermions,

$$S_F^{\mathrm{eff}}[\psi^\dagger, \psi; b^\dagger, b] = S_F^0[\psi^\dagger, \psi; b^\dagger, b] + \frac{1}{2} \sum_{\mathbf{r},\tau} \left[\psi_\uparrow^\dagger \psi_\uparrow \psi_\downarrow^\dagger \psi_\downarrow - \psi_\uparrow^\dagger \psi_\uparrow b^\dagger b - \psi_\downarrow^\dagger \psi_\downarrow b^\dagger b \right]. \tag{3.1}$$

Here the second term in Eq.(3.1) can be rewritten as $(1/4)\sum_{\mathbf{r},\tau} n^2(\mathbf{r},\tau)$, where the local charge density $n = \sum_f \psi_f^\dagger \psi_f - b^\dagger b$. Since we are left with the temporal difference terms with ∂_τ^+, the effective action can be rewritten by the Hamiltonian formalism,

$$H_F^{\mathrm{eff}} = H_F^0 + \frac{1}{4a_\tau} \sum_{\mathbf{r}} n^2(\mathbf{r}). \tag{3.2}$$

This effective Hamiltonian can be regarded as a repulsive Hubbard model, which favors charge neutrality, i.e. $\sum_f \psi_f^\dagger \psi_f - b^\dagger b = 0$, for each lattice site. The effective coupling constant appears as $U_{\mathrm{eff}} = 1/4a_\tau$.

In the continuous-time limit $a_\tau \to 0$, the local charge neutrality is strongly required due to the infinitely strong Hubbard repulsion $U_{\mathrm{eff}} \to \infty$, which fixes one electron for each site. This is the straightforward consequence of the absence of photon propagation, which can be reproduced in the continuum limit $(a \to 0)$ as well; the coupling between the fermions and the photons is given by the exponential factor $\exp[-\int d\tau d^3\mathbf{r}\ i A_0(\mathbf{r},\tau) n(\mathbf{r},\tau)]$ in the path integral formalism. Integrating out the photon degrees of freedom (A_0), we are left with delta functions, $\prod_{\mathbf{r},\tau} \delta(n(\mathbf{r},\tau))$, which is exactly the "local charge neutrality" condition. Since the hopping of electrons is prohibited under the local charge neutrality, the system becomes a Mott insulator.

[2] In other words, the spatial components are quite weakly coupled, which should be treated by weak-coupling expansion.

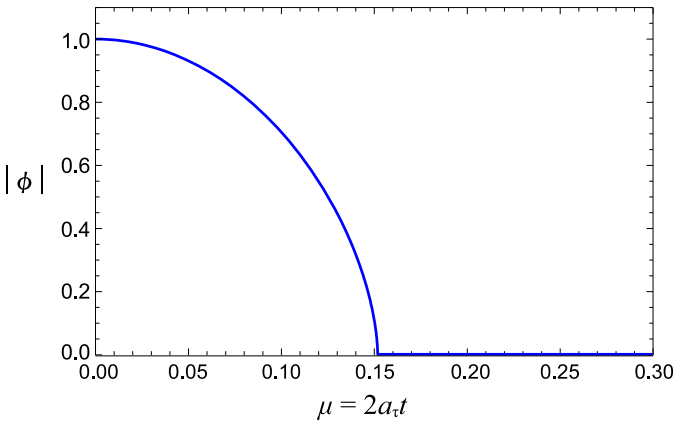

Figure 1: The behavior of the magnitude of the antiferromagnetic order (Neél vector) $|\boldsymbol{\phi}|$ as a function of the parameter $\mu = 2a_\tau t = (a_\tau/a)v_F$, in 3D $(d = 3)$. The order parameter saturates in the continuous-time limit $a_\tau \to 0$, and vanishes at the critical value $\mu_c = 0.152$.

The Mott transition discussed here can be directly observed by focusing on the order parameter under the mean-field analysis. It is well known that the ground state of the strong Hubbard repulsion is antiferromagnetism, characterized by the Neél vector, $\boldsymbol{\phi}(\mathbf{r},\tau) = (-1)^{(r_1+\cdots+r_d)/a}\langle\psi^\dagger\boldsymbol{\sigma}\psi\rangle(\mathbf{r},\tau)$, where $\boldsymbol{\sigma}$ is the 2×2 Pauli matrix. Taking the Neél vector as a mean field, we can easily integrate out the fermionic degrees of freedom, to obtain the effective potential (free energy) of the system as a function of $\boldsymbol{\phi}$,

$$F_{\rm eff}(\boldsymbol{\phi}) = -\frac{1}{\beta N^3}\ln Z(\boldsymbol{\phi}) = \frac{1}{12a_\tau}|\boldsymbol{\phi}|^2 - \frac{1}{a_\tau N^3}\sum_{\mathbf{q}}\varepsilon(\boldsymbol{\phi};\mathbf{q}), \tag{3.3}$$

where the summation over the Matsubara frequency ω_n is taken at zero temperature. Here $\varepsilon(\boldsymbol{\phi};\mathbf{q}) = \left[|\boldsymbol{\phi}/6a_\tau|^2 + (2t)^2\sum_j\cos^2(aq_j)\right]^{1/2}$ is the single-particle energy of electron under the mean field $\boldsymbol{\phi}$, which opens a mass gap for finite $\boldsymbol{\phi}$. The expectation value of the Neél vector $\boldsymbol{\phi}$ corresponds to the minimum of the free energy in Eq.(3.3). This minimum depends on the single parameter $\mu \equiv 2a_\tau t = (a_\tau/a)v_F$, whose behavior in 3D $(d = 3)$ is shown in Fig. 1. The magnitude of the Neél vector $|\boldsymbol{\phi}|$ saturates at the continuous-time limit $a_\tau = 0$, monotonically decreases as μ increases, and vanishes at the critical value $\mu_c = 0.152$ at the mean-field level.

We can check that this result can be related to the previous strong-coupling analysis in 3D Dirac semimetals [9]; the lattice spacings in that analysis are fixed as $a_\tau/a = v_F^{-1}$, so that the lattice should be hyper-cubic in the spacetime under the scale transformation $\tau \mapsto \tau/v_F$. This corresponds to the parameter μ fixed at 1 in the present argument, where $|\boldsymbol{\phi}|$ completely vanishes and the system becomes gapless, in agreement with Ref. [9].

4. Lattice anisotropy

So far we have employed the lattice with a cubic symmetry. In realistic 3D Dirac semimetals, however, there exists a lattice anisotropy distinguishing one axis from the other, due to the layered structure in the synthesis process. Here we introduce an anisotropy in the nearest-neighbor

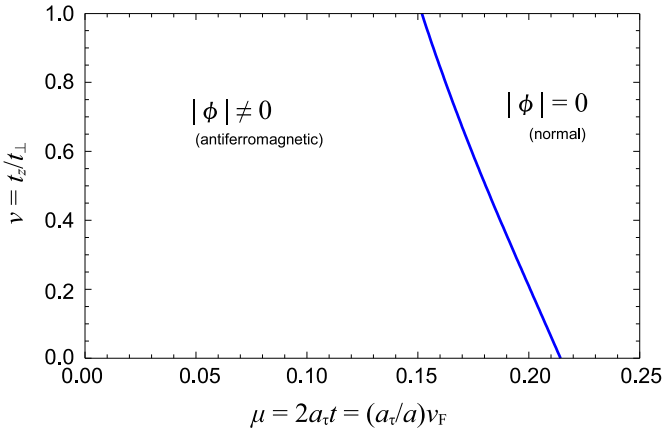

Figure 2: The phase diagram characterizing the presence ($\phi \neq 0$) or the absence ($\phi = 0$) of the antiferromagnetism (Neél order), parametrized by $\mu = (a_\tau/a)v_F$ and $\nu = t_z/t_\perp$. The system is antiferromagnetic in the continuous-time limit ($\mu = 0$), independently of the dimensionality parameter ν.

hopping amplitude t; we define the hopping amplitudes in the z- and x/y-directions as t_z and $t_\perp$, respectively, and denote their ratio by the dimensionless parameter $\nu = t_z/t_\perp$. ν characterizes the "dimensionality" of the system: if $\nu = 1$, the lattice is perfectly (spatially) 3D-cubic, reproducing the properties discussed in the previous section. On the other hand, if $\nu = 0$, there is no hopping in the z-direction, and the system becomes just an ensemble of 2D slabs stacked on top of one another. Thus $\nu \in (0,1)$ characterizes the "intermediate" state between 2D and 3D.

Following the process of mean-field analysis in the previous section, we can estimate the mean-field expectation value of the Neél vector (antiferromagnetic order parameter) $|\phi|$ in the strong-coupling and zero-temperature limit, as a function of the parameters μ and ν. Taking $\mu = (a_\tau/a)v_F$ and $\nu = t_z/t_\perp$ as control parameters, we obtain a phase diagram characterizing the presence or absence of the antiferromagnetism ϕ, as shown in Fig. 2. We can see that the system always shows the antiferromagnetism in the continuous-time limit $\mu \propto a_\tau = 0$, independently of the dimensionality, which is indeed the consequence of the infinitely strong Coulomb interaction, i.e. the photon-mediated electron correlation in the strong-coupling limit. The dimensionality-dependent phase transition observed in Ref. [9] can be understood as an artifact of the finite lattice spacing in the temporal direction, which moderates the infrared singularity at $\phi = 0$.

5. Summary

In this work, we have observed the electron correlation effects in 3D Dirac semimetals, by using the strong coupling expansion of lattice gauge theory. We have improved the discretization of the imaginary time by employing the forward difference instead of the forward-backward difference, to investigate the lattice spacing (a_τ-) dependence and to meet the path-integral formalism correctly. We have also introduced the field of the positive background charge, coming from the positive ions sitting at each lattice site.

In the strong-coupling limit, the integration over the gauge field generates a strong on-site (Hubbard) repulsion of fermions, leading to an antiferromagnetic order and opening a bandgap at the Dirac nodes. Such a strong Hubbard repulsion originates from the local charge neutrality required by the coupling to the gauge field, which can be reproduced in the continuum limit. By introducing an anisotropy in the hopping amplitudes (or the Fermi velocity), we have found that the antiferromagnetic order appears independently of the anisotropy in the continuous-time limit, i.e. there arises a bandgap either in 2D or 3D limits.

The analysis in the continuous-time limit here shows a clear difference with the previous strong-coupling analysis using the staggered fermion formalism [9], where the antiferromagnetic order vanishes in 3D and appears in the intermediate state between 2D and 3D. Such a behavior can be understood as an artifact of the discretization of time, since it can be reproduced by taking the temporal lattice spacing a_τ comparable to a/v_F, i.e. away from the continuous-time limit. Although it is unphysical to take a_τ finite, it still serves as an effective method to introduce the screening effect of Coulomb interaction, since it reduces the strength of the on-site repulsion and moderates the infrared singularity at zero-momentum in the one-loop self-energy of the fermions.

The strong-coupling analysis performed here is a starting point for exploring the finite-coupling regime, away from the strong-coupling limit. Finite-coupling regime can be reached by the strong-coupling expansion, namely the power series expansion by the inverse coupling constant g^{-1} around the strong-coupling limit $g^{-1} = 0$. Finite g^{-1} enables the photon propagation, which correlates the charge densities at different lattice sites; thus it may modify the electron correlation properties non-locally, leading to the renormalization of the Fermi velocity v_F as well as the reduction of the bandgap. It remains an important question to compare the renormalization group flow of v_F from the strong-coupling limit with that from the weak-coupling limit, suggested in previous literatures.

Acknowledgments

The author thanks Kentaro Nomura and Akihiko Sekine for fruitful discussions. This work was supported by JSPS Grant-in-Aid for Research Activity Start-up (No. 15H06023).

References

[1] S. M. Young, S. Zaheer, J. C. Y. Teo, C. L. Kane, E. J. Mele, and A. M. Rappe, Phys. Rev. Lett. **108**, 140405 (2012).

[2] K. S. Novoselov *et al.*, Science **306**, 666 (2004).

[3] Z. K. Liu *et al.*, Science **343**, 864 (2014).

[4] Z. K. Liu *et al.*, Nat. Mater. **13**, 677 (2014).

[5] Q. Li *et al.*, arXiv:1412.6543.

[6] G. L. Yu *et al.*, P. Natl. Acad. Sci. USA **110**, 3282 (2013).

[7] J. Hofmann, E. Barnes, and S. Das Sarma, Phys. Rev. B **92**, 045104 (2015).

[8] R. E. Throckmorton, J. Hofmann, E. Barnes, and S. Das Sarma, Phys. Rev. B **92**, 115101 (2015),

[9] A. Sekine and K. Nomura, Phys. Rev. B **90**, 075137 (2014).